

Comparative Analysis of Existing and Proposed Deep Learning Models for Brain Tumor Detection in MRI

Vivek Kumar Gupta
Department of Computer Science and
Engineering
Medicaps University, Indore, India
guptav06@gmail.com

Suresh Jain
Department of Computer Science and
Engineering
Medicaps University, Indore, India
suresh.jain@rediffmail.com

Kailash Chandra Bandhu
Department of Computer Science and
Engineering
Medicaps University, Indore, India
kailashchandra.bandhu@gmail.com

Abstract - Detecting brain tumors by MRI is a sensitive activity in medical image analysis where, an early and precise diagnosis can be important to the treatment of patients. In this paper, the researcher will conduct a comparative study of the existing models of deep learning and a proposed deep learning model, which classifies brain tumors. The aim is to assess the performance of various CNN models in accuracy, generalization and interpretations on diverse MRI data. The two publicly available datasets, Figshare and BraTS 2020, are used as the methodology to provide cross-dataset validation. A number of deep learning architectures, such as VGG16, ResNet50, AlexNet and EfficientNetB0 are executed and compared to a proposed lightweight LeNet model with Squeeze-and-Excitation (SE) attention blocks. To make a fair comparison, a standardized preprocessing pipeline (resizing, normalization, and data augmentation) is used. Also, explainable AI methods like Grad-CAM and LIME are employed to enhance model interpretability and clinical transparency. The findings indicate that traditional models are reasonably effective in classification tasks but have problems of generalization and feature discrimination. Conversely, the suggested LeNet + SE model has better feature representation, enhanced attention to tumor-relevant areas, and higher accuracy on the BraTS2020 dataset. In general, the given framework offers a more effective, efficient, and interpretable brain tumor detection solution than the current ones.

Keyword- Brain Tumor Detection ,Deep Learning, MRI Classification, Convolutional Neural Networks(CNN) and Squeeze-and-Excitation(SE) Blocks.

I. INTRODUCTION

The detection of brain tumor through magnetic resonance imaging (MRI) has emerged as a key study area in medical image analysis because of its paramount importance in early detection, treatment planning and enhancing patient outcomes. As the field of artificial intelligence is rapidly expanding, automatic classification of brain tumors using deep learning-based techniques became popular. Such techniques minimize the necessity of manual feature extraction and aid radiologists with quicker and more reliable diagnostic aid. VGG16, ResNet50, AlexNet and EfficientNet are examples of convolutional neural networks (CNNs) that have been widely employed in the existing literature in classifying brain tumor images because they are good at learning hierarchical image features.[1], [2], [3].

Although existing studies have shown promising results, most of them still face several limitations. A major issue is that many models are trained and evaluated on a single dataset, which reduces their ability to generalize across different clinical environments. Medical MRI data often varies due to differences Generalization in scanners, imaging protocols and patient conditions makes generalization a problem. Besides this, most of the existing methods are based on deep architectures which are computationally expensive and may not be applicable to real-time medical practice. The other weakness is that typical CNN models do not have attention mechanisms, i.e. they do not pay special attention to tumor-specific regions of the image, and may fail to target them. Moreover, interpretability is also an issue, most deep learning models are black-box models, making their use in clinical practice more difficult.[4], [5], [6], [7].

To handle these problems, the proposed research is dedicated to the detection of brain tumor with the help of a medical image classification framework based on deep learning and conducts a systematic comparison of the existing models with the proposed one. The paper assesses several popular CNN models, which were utilized in previous studies, as well as compares their results with the performance of a newly developed proposed architecture that incorporates a lightweight CNN model with attention-based feature enhancement. This is done in a comparative manner involving a common experimental design to promote fairness and consistency in the assessment [8], [9].

In order to cope with these issues, the proposed study is devoted to the identification of brain tumor through the use of a medical image classification framework that provides the assistance of deep learning and performs a systematic comparison between the existing models and the suggested one. The paper evaluates various famous CNN models, that have been used in prior research, and compares their performance to that of a recently designed proposed architecture, that uses a lightweight CNN model with attention-based feature enhancement. This is done comparatively with a shared experimental design to encourage equity and uniformity in the evaluation [10], [11], [12], [13]. The proposed methodology will enhance the features representation thanks to the attention to more pertinent areas of tumor and minimized redundant computation complexity. Through the introduction of the systematic comparison between the traditional CNN-based methods and the proposed enhanced

model, the study will focus on the strong and weak points of the current methods and illustrate the gains provided by the propose.[14], [15], [16], [17].

In general, the study will add to the body of medical image analysis, offering a comparative assessment of current and suggested deep learning techniques of detecting brain tumors, with the aim of creating a more resistant, effective, and clinically viable classification system.

II. LITERATURE REVIEW

Jia & Chen, 2025[18] present a fully automatic algorithm of cerebral venous segmentation of the MRI based on structural and morphological features. It utilized probabilistic neural networks and gave the system 98.51% accuracy with regard to the detection of abnormal tissues.

Devi et al., 2025[19] created a brain tumor detector with convolution-2D and batch normalization in deep learning. The tumor detection in MRI images was performed, and precision, recall, and F1-score performance were enhanced.

Vandana et al., 2023[20] trained a CNN-based brain tumor classification model on MRI images. Data augmentation together with pretrained ResNet50 and EfficientNet enhanced the classification performance of tumor and non-tumor classes.

Aggarwal et al., 2023[21] offers a better ResNet framework of brain tumor segmentation. The technique enhanced projection shortcuts and residual connections, and it was more accurate, recalled more, and cost less to compute.

Ravinder et al., 2023[22] present a hybrid CNN-GNN architecture to classify brain tumors with the help of graph convolution and adjacency matrices. The Net-2 model had the best accuracy of 95.01.

TABLE I. LITERATURE SUMMARY

| Author / Year | Method | Results | Research Gap |
|-------------------------|--|---|--|
| Shah et al., 2022[23] | Fine-tuned EfficientNet-B0 deep CNN model with image enhancement and data augmentation for brain tumor classification using MRI images. | Achieved high classification accuracy of 98.87% and outperformed other CNN models such as VGG16, InceptionV3, Xception, and ResNet50. | The study focuses only on deep learning models and does not combine handcrafted features or attention mechanisms for improved feature representation. |
| Khan et al., 2022[24] | Hierarchical Deep Learning-Based Brain Tumor (HDL2BT) classification using CNN for multi-class brain tumor classification including glioma, meningioma, pituitary, and no-tumor classes. | Achieved 92.13% precision with improved classification performance compared to traditional methods. | The model uses hierarchical CNN but does not integrate texture features, keypoint features, or attention mechanisms to enhance classification performance. |
| Rizwan et al., 2022[25] | Proposed Gaussian Convolutional Neural Network (GCNN) for multi-class brain tumor classification using MRI datasets. | Achieved 99.8% and 97.14% accuracy on two different datasets for brain tumor classification. | The study focuses only on deep CNN architecture and does not use hybrid feature extraction methods such as GLCM or ORB or attention mechanisms. |
| Gaur et al., | CNN model combined with explainable AI | Achieved classification | The study focuses on interpretability |

| | | | |
|-----------------------|---|--|---|
| 2022[26] | techniques such as LIME and SHAP for interpretable brain tumor classification. | accuracy of 94.64% and improved interpretability of deep learning model predictions. | but does not combine handcrafted features and attention mechanisms for improving classification accuracy. |
| Asif et al., 2022[27] | Transfer learning models such as Xception, DenseNet, InceptionResNetV2, and NASNet for brain tumor classification using MRI images. | Xception model achieved highest accuracy of 99.67% on MRI-large dataset and 91.94% on MRI-small dataset. | The study focuses only on transfer learning models and does not integrate hybrid feature extraction or attention-based feature selection methods. |

III. PROPOSED METHODOLOGY

This paper proposes a comparative deep learning model to classify brain tumors with multi-source MRI images with an emphasis on robustness, generalization, and interpretability. In contrast to the current work that is done with the help of one dataset or one model, it considers cross-dataset validation, a variety of CNNs, and the attention-based learning to address the major shortcomings of the existing ones. The research involves the two heterogeneous datasets, Figshare and BraTS2020, with different levels of complexity and imaging features, which allows successfully testing the model generalization. It also compares various architectures, such as VGG16, ResNet50, AlexNet, EfficientNetB0, and a lightweight LeNet with Squeeze-and-Excitation (SE) attention blocks, comparing both the classical and the more modern deep learning models. All models are trained using the standardized preprocessing and training setup to allow comparison and reproducibility. Also, explainable AI methods, like Grad-CAM and LIME, are employed to enhance model interpretability and clinical trust, the approach emphasizes cross-dataset learning, attention-enhanced lightweight modeling, and explainability to create a more robust and clinical-relevant brain tumor classification system.

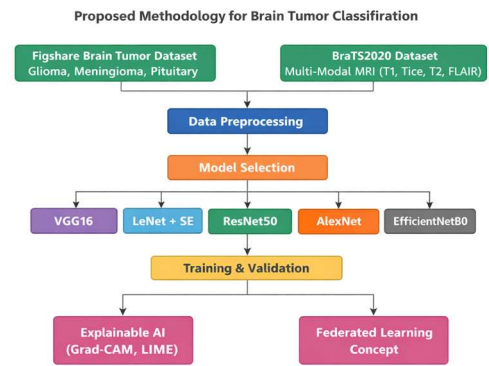


Fig 1. Proposed Flow Chart

A. Data collection

This study uses two publicly available brain MRI datasets: the Figshare Brain Tumor Dataset

<https://www.kaggle.com/datasets/rahimanshu/figshare-brain-tumor-classification> and the BraTS2020 (Brain Tumor Segmentation Challenge 2020) dataset,

<https://www.kaggle.com/datasets/rahimanshu/brats2020-brain-tumor-classification> validation of the proposed models.

Figshare dataset is a collection of MRI images which are divided into three tumor types: Glioma, Meningioma, and Pituitary tumors. Such images are marked and saved in different folders, thus appropriate in supervised deep learning activities. The dataset exhibits variability in tumor shape, size and intensity which is representative of real clinical situations and is popular in research because of its accessibility and consistency.

BraTS2020 dataset is a more intricate, multi-institutional, multi-modal dataset with MRI scans that include T1, T1ce, T2, and FLAIR. It is used in segmentation but it is modified in this case to do classification to test the generalization of the model. Its great heterogeneity in imaging conditions and tumor characteristics offers a demanding testing environment to test model robustness and provides cross-dataset performance testing in brain tumor classification.

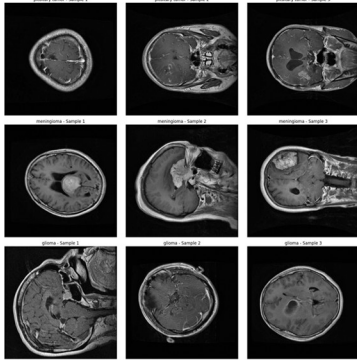


Fig 2. Sample images from each category in the Fig share dataset before preprocessing

Figure 2 An example of pre-preparation MRI images of each group of tumours across the dataset is provided in figure 2. These rough pictures denote how the size, shape, texture and location of the tumour can vary and therefore highlight the difficulty in identifying brain tumours. Follow-up application of preprocessing methods contributes to increased performance of images and models.

B. Data Preprocessing

A good preprocessing is needed in preparation of the data to be trained in the model. The raw MRI images were first preprocessed and this helped to normalise the data and enhance the model performance. The name of the labels and the paths to each JPG image have been initially derived automatically as part of their directory structure. Then, the photos were all converted to grayscale and key data about texture and intensity were stored, which reduced the complexity of inputs and low computing cost. The second was to downsize the images to 224 x 224 pixels, the typical dimensions of pre-trained multilayer neural networks like VGG-16. In order to obtain some form of consistency and stabilisation of the learning the model process, the pixel values were rescaled to the [0, 1] range after being rescaled between 255. To ensure the proportion of classes remains the same in the subsets we have used stratified sampling to split the data into half: 80% train and 20% test. After the preprocessing had been completed, intensity distribution graphs were plotted and sample photographs were prepared to observe the normalization using the naked eye. The final image is of shape (224, 224, 1). This homogeneous and monotonous preprocessing is significant to minimize biasing because of the various image format or lighting conditions to ensure that the deep learning model learns meaningful patterns.

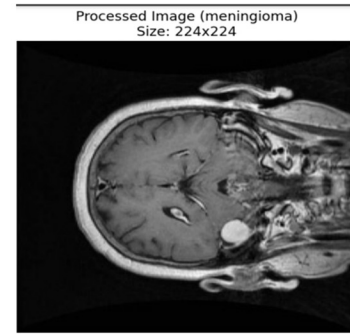


Fig 3. Random sample image after resizing and normalizing the images of Figshare Data:

Figure 3 shows a randomly chosen MRI image that has been resized and normalized. Normalization is used to make sure that the scale of pixel intensity is always in a fixed range and resizing is used to make sure that the size of the images in the set is constant. These preprocessing are significant in enhancing the model efficiency, accuracy of training and lowering the cost of computing in the classification.

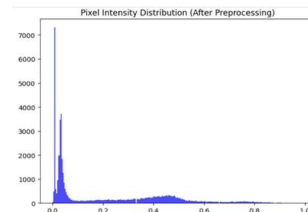


Fig 4. Image pixel intensity distribution plot (after preprocessing)

Figure 4 shows a randomly chosen MRI image that has been resized and normalized. Normalization is used to make sure that the scale of pixel intensity is always in a fixed range and resizing is used to make sure that the size of the images in the set is constant. These preprocessing are significant in enhancing the model efficiency, accuracy of training and lowering the cost of computing in the classification.

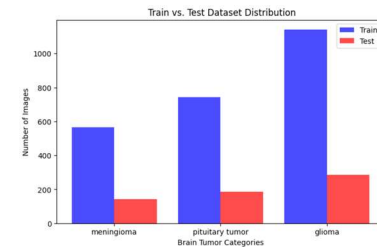


Fig 5. Dataset distribution after train-test split

Figure 5 is used to show the dataset that is split into train-test. This graph is associated with the placement of the photos in training and testing sets in the event of each type of tumour. The deep learning model will be trained and tested fairly through a balanced distribution that will minimize the chances of bias or overfitting.

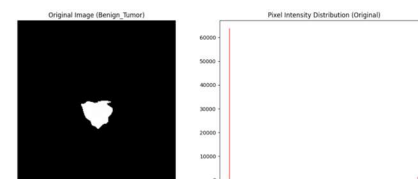


Fig. 6 Pixel intensity distribution of a benign tumor sample from the BraTS2020 dataset.

The localized intensity of the benign tumor is seen in the image, the high background and low high-intensity tumor pixels are seen in the histogram.

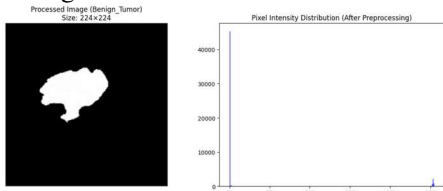


Fig. 7 Preprocessed benign tumor image and corresponding pixel intensity distribution from the BraTS2020 dataset.

Preprocessing with normalization of intensities and image resizing makes the tumors visible and lessens the importance of the background, which would result in more successful and reliable deep learning training.

C. Model Implementation

- VGG16 Model:** VGG16 was tested with transfer learning with pretrained ImageNet weights to classify brain tumors on Figshare and BraTS2020 datasets. The initial fully connected layers were substituted with a bespoke classification head with global average pooling and dense layers. Input images were rescaled, normalized and augmented (rotation, inversion, scaling) to enhance generalization. Adam optimizer was used to train the model and standard classification metrics evaluated the performance. Additional layers were fine-tuned to fit features to medical images.
- LeNet + SE Model:** A LeNet-style architecture was optimized to be lightweight and was extended with Squeeze-and-Excitation (SE) blocks to recalibrate channel-wise features. The model isolates low- and mid-level features, and SE modules enhance attention to tumor-relevant areas. The model was then trained with Adam optimizer and cross-entropy loss in addition to regularization to minimize overfitting after preprocessing (resizing and normalization). Although it is simple, the attention mechanism can enhance low-cost feature discrimination.
- ResNet50 Model:** The transfer learning was done with ResNet50 using ImageNet weights. Its leftover interactions assist it in overcoming the problem of vanishing gradients and in learning deep features. The last classification layers were substituted with a custom head comprising of global average pooling and dense layers. Resizing, normalization, and augmentation were used to preprocess the images. Adam optimizer and cross-entropy loss were used to fine-tune the chosen layers to achieve stable training and better generalization.
- AlexNet Model:** AlexNet was used as a slightly deep CNN that included five convolutional and fully connected layers. It uses ReLU activation and max pooling to capture coarse-to-fine features. The overfitting was minimized by dropout and the model was trained using Adam optimizer and cross-entropy loss. AlexNet is also suitable and effective in terms of training and performance in MRI-based classification, although it has a simpler architecture.
- EfficientNetB0 Model:** Compound scaling was applied to EfficientNetB0 to balance the depth, width and resolution.

A pretrained model was fine-tuned with a replacement of the classification head with the custom dense layers. Images as inputs were resized, normalized and augmented. Adam optimizer and loss by cross-entropy were used to train. It was a scalable baseline model, although its performance was variable depending on the complexity of the data and domain adaptation constraints, and it was computationally efficient.

TABLE II. HYPER PARAMETER DETAILS

| Hyperparameter | VGG16 | LeNet + SE | ResNet50 | AlexNet | EfficientNetB0 |
|------------------------|---------------------------------------|---------------------------------------|---------------------------------------|---------------------------------------|---------------------------------------|
| Dataset | Figshare, BraTS2020 | Figshare, BraTS2020 | Figshare, BraTS2020 | Figshare, BraTS2020 | Figshare, BraTS2020 |
| Input Image Size | 224 × 224 × 3 | 224 × 224 × 3 | 224 × 224 × 3 | 224 × 224 × 3 | 224 × 224 × 3 |
| Model Initialization | ImageNet Pretrained | Random Initialization | ImageNet Pretrained | Random / Pretrained | ImageNet Pretrained |
| Convolution Layers | 13 | 2 + SE Blocks | 49 + Residual Blocks | 5 | MBCConv Blocks |
| Attention Mechanism | None | Squeeze-and-Excitation (SE) | None | None | Built-in (MBCConv) |
| Pooling Strategy | Max + Global Avg Pool | Max Pool | Global Avg Pool | Max Pool | Global Avg Pool |
| Fully Connected Layers | Custom Dense Layers | Dense Layers | Custom Dense Layers | Dense Layers | Custom Dense Layers |
| Activation Function | ReLU | ReLU | ReLU | ReLU | Swish |
| Output Activation | Sigmoid / Softmax | Sigmoid | Sigmoid / Softmax | Sigmoid | Sigmoid |
| Loss Function | Binary Cross-Entropy | Binary Cross-Entropy | Binary Cross-Entropy | Binary Cross-Entropy | Binary Cross-Entropy |
| Optimizer | Adam | Adam | Adam | Adam | Adam |
| Learning Rate | 0.0001 | 0.0001 | 0.0001 | 0.0001 | 0.0001 |
| Batch Size | 16 / 32 | 16 / 32 | 16 / 32 | 16 / 32 | 16 / 32 |
| Number of Epochs | 20–30 | 20–30 | 20–30 | 20–30 | 20–30 |
| Dropout Rate | 0.5 | 0.5 | 0.5 | 0.5 | 0.5 |
| Data Augmentation | Rotation, Flip, Zoom | Rotation, Flip | Rotation, Flip, Zoom | Rotation, Flip | Rotation, Flip, Zoom |
| Fine-Tuning | Yes (Top Layers) | No | Yes (Last Blocks) | No | Yes (Top Layers) |
| Evaluation Metrics | Accuracy, Precision, Recall, F1-score | Accuracy, Precision, Recall, F1-score | Accuracy, Precision, Recall, F1-score | Accuracy, Precision, Recall, F1-score | Accuracy, Precision, Recall, F1-score |

III. RESULT & COMPARISON

TABLE III. RESULTS OF PROPOSED MODELS ON FIGSHARE DATA

| Model | Accuracy | Precision | Recall | F1-score |
|----------------|----------|-----------|--------|----------|
| VGG16 | 93.31 | 37.11 | 37.19 | 37.15 |
| ResNet50 | 93.31 | 35.77 | 35.89 | 35.83 |
| AlexNet | 89.89 | 36.07 | 34.91 | 35.41 |
| EfficientNetB0 | 46.88 | 21.97 | 46.88 | 29.92 |
| LeNet+SE | 61.17 | 35.81 | 32.14 | 32.10 |

The Figshare dataset has the highest accuracy of VGG16 and

ResNet50 (93.31), representing a good overall performance in classification. Both models however exhibit low precision, recall and F1-scores indicating that they are incapable of identifying all the classes and also dealing with class imbalance. AlexNet has a slightly lesser accuracy (89.89) with equally low F1-score, whereas EfficientNetB0 has low accuracy (46.88) despite a high recall, which is an over-prediction of positive cases. LeNet has an average accuracy of 61.17. In general, VGG16 is the most balanced model in this dataset of all models.

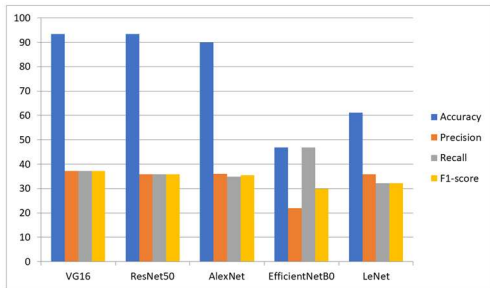


Fig. 8 Performance Evaluation Graph of Proposed Models on Figshare Dataset

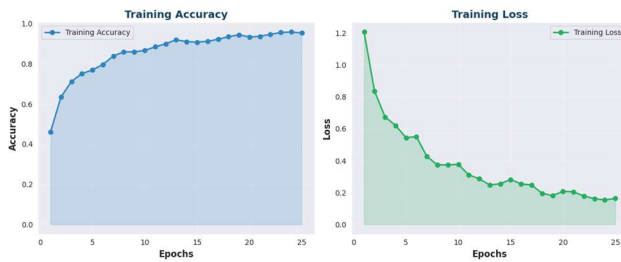


Fig. 9 Training Accuracy and Loss Graph
 Confusion Matrix - Brain Tumor Classification

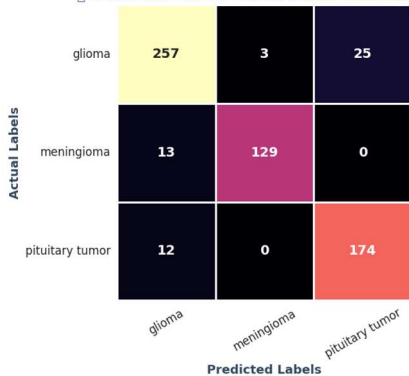


Fig. 10 Confusion Matrix of VGG16

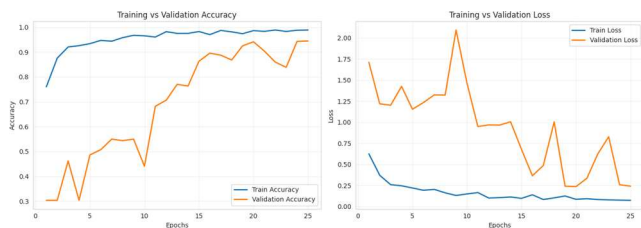


Fig. 11 Training vs Validation Accuracy and Loss of Resnet 50

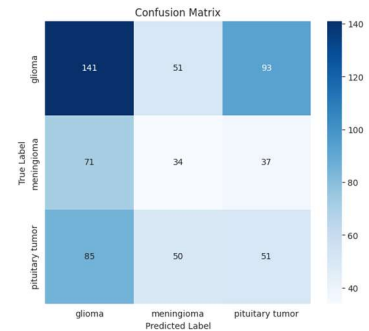


Fig. 12 Confusion Matrix of ResNet50

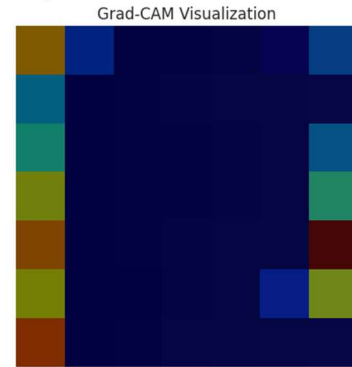


Fig. 13 Grad-CAM Visualization on Figshare data

Grad-CAM visualization was used to examine the Figshare dataset to understand which parts of the image create the most significant effect on the decisions of the model to categorize them as either benign or malignant. The heatmaps created are warm (yellow, red) and cold (blue, dark colors), where those with a substantial contribution to the prediction of the model are displayed, and those with low or no contribution are displayed, respectively. The large dark-blue region is positioned in the middle of the images implying that much attention was not paid to the central image appearances by the model and the central pixels were of minor importance in the final decision. Overall, as the outputs of the Grad-CAM show, the model is focused more on the edges of the image than on the tumor area in the center of the image. This tendency implies that a potential dependence on peripheral image features or acquisition artifacts, and more vigorous efforts towards ensuring the utilization of clinically significant features would involve region-specific learning strategies and more vigorous preprocessing strategies.

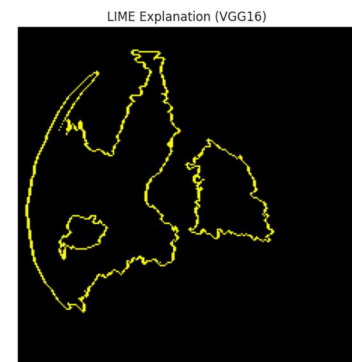


Fig.14 LIME

According to the LIME description of the VGG16 model, the largest areas of superpixels are mostly concentrated along the edges of the structural features, which indicates that the model is

generally reliant on the form and edge-related features in the procedure of differentiating the benign and the malignant tumors. It is localization in space but the center of the tumor is not completely concentrated in the model and it can be assumed that the concentration is based on the image characteristics in the context rather than on the concentration of the tumor itself. It must be noted that tumor segmentation was not performed in the provided study since there had been no pixel-level annotations in the dataset and therefore, the research study was conducted on an image-level classification with the segmentation being a guideline to the further study. In addition, a federated learning architecture is conceptually proposed to solve the problem of data privacy and ethical concerns in medical imaging so that each hospital can train a local model using the assistance of private MRI data and only sends the weights of the learned models to a central server, which averages them via Federated Averaging (FedAvg), and hence learns together without exposure to raw patient data.

TABLE IV. RESULTS OF PROPOSED MODELS ON BRATS2020 DATA

| S. No. | Model | Accuracy | Precision | Recall | F1-Score |
|--------|----------------|--------------|--------------|--------------|--------------|
| 1 | VGG16 | 93.48 | 93.10 | 93.48 | 92.85 |
| 2 | LeNet + SE | 98.44 | 98.43 | 98.44 | 98.43 |
| 3 | ResNet50 | 94.45 | 94.22 | 94.45 | 94.29 |
| 4 | AlexNet | 97.58 | 97.56 | 97.58 | 97.57 |
| 5 | EfficientNetB0 | 93.00 | 91.00 | 73.00 | 79.00 |

The results indicate that LeNet + SE model is the most effective one in relation to all of the evaluation measures that reflect the efficiency of squeeze-and-excitation blocks to enhance feature representation. ResNet50 and VGG16 are also competitive and have lower comparatively better scores than AlexNet. The recall and F1-score of EfficientNetB0 are low indicating that the model can only identify malignant cases with BraTS2020.

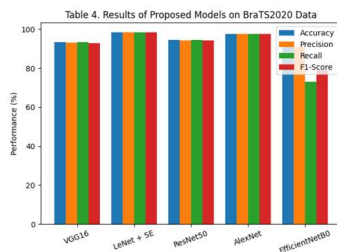


Fig.15 Performance Evaluation Graph

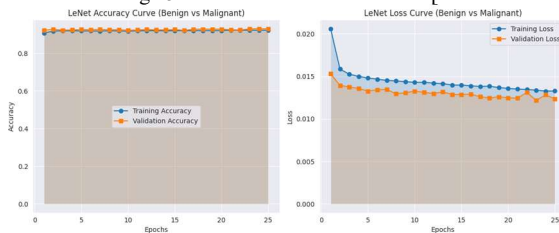


Fig.16 Accuracy and Loss curve of LeNet+SE

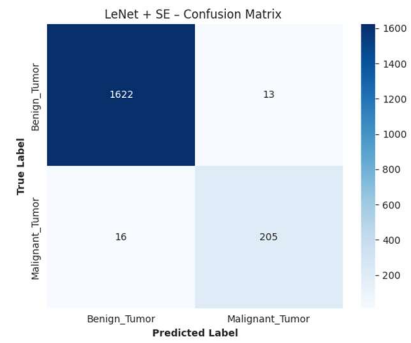


Fig 17 Confusion Matrix of LeNet +SE

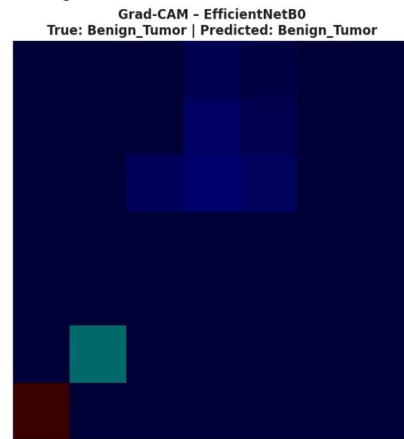


Fig 18. Grad-CAM (EfficientNetB0) Brat2020 data

With such Grad-CAM visualization, it is possible to observe the localities of the MRI image of Brat2020 data, which has presumably altered the choice of the EfficientNetB0 model. The model gave the appropriate label Benign Tumor to the sample as indicated by the agreement between the actual and the predicted labels. The identified areas represent spatial areas that the network focused its attention on and prediction was made. The fact that the activation was relatively localized and mild intensity suggests that the model was anchored on subtle and localized structural properties and not the aggressive and extensive abnormality patterns, which is also consistent with the nature of benign tumors. This visualization increases the interpretability of models because it is effective in showing that the regions of an image that are relevant to medicine are being used to make a prediction rather than random background data.

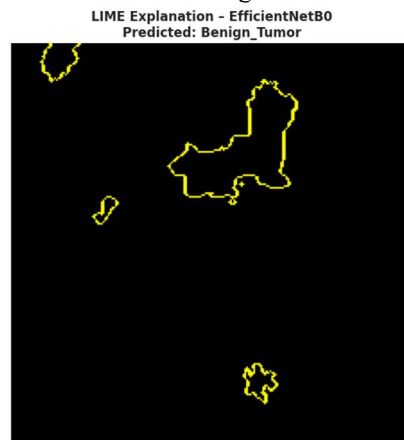


Fig. 19. LIME (EfficientNetB0) of Brat2020 data

This LIME description reveals specific regions of the image that most affected the EfficientNetB0 model prediction of Benign Tumor of Brat2020. The superpixels are filled with yellow and indicate the localities, which have had a good influence on the

classification decision. This is the connection which these areas are linked to localized structural patterns in the MRI image that the model is highly sensitive in the characterization of benign properties. The observation that there are no large highlighted areas, suggests that the model was done on few

meaningful features as opposed to the noise or background areas. Altogether, this visualization makes the interpretation process easier as it illustrates that the prediction is guided by the parts of images that used to be relevant, and it is more difficult to doubt the model decision-making process.

TABLE V. COMPARATIVE ANALYSIS OF EXISTING WORK VS PROPOSED WORK

| Study | Methodology | Dataset | Models Used | Key Limitation | Interpretability | Evaluation Focus | Proposed Work Advantage |
|--------------------------------|--|-----------------------|--|-----------------------------------|-----------------------|--|---|
| Ahmed et al., 2023[28] | AI-based brain disease analysis review | General MRI datasets | Various AI/ML models | Limited datasets, black-box issue | Low | Conceptual analysis | Uses cross-dataset validation + explainability |
| Yousef et al., 2023[29] | U-Net based segmentation study | BraTS 2020 | 3D U-Net, Attention U-Net | Focus only on segmentation | Moderate | Dice, Hausdorff distance | Performs classification + segmentation insights |
| Martucci et al., 2023[30] | MRI-based diagnostic analysis | Clinical MRI data | Conventional + AI methods | Limited deep learning comparison | Moderate | Clinical interpretation | Adds deep learning comparative framework |
| Venmathi et al., 2023[31] | CNN-based classification | MRI dataset | VGG-19 based DCNN | Single architecture dependency | Low-Moderate | Accuracy-based | Uses multiple CNN + attention model |
| Shawon et al., 2023[32] | Automated classification | Balanced MRI datasets | NASNet, EfficientNet, ResNet | Dataset imbalance sensitivity | Moderate | Accuracy, recall | Adds cross-dataset robustness + SE attention |
| Existing CNN Studies (General) | Deep learning classification | Single dataset | VGG16, ResNet, etc. | Poor generalization | Low | Accuracy only | Multi-dataset + fair comparison |
| Proposed Work | Comparative deep learning framework | Figshare + BraTS2020 | VGG16, ResNet50, AlexNet, EfficientNetB0, LeNet+SE | Overcomes existing limitations | High (Grad-CAM, LIME) | Accuracy, Precision, Recall, F1 + interpretability | Cross-dataset + attention-based + explainable + fair comparison |

The proposed work is superior to existing studies because it is free of critical limitations like dependency on single dataset, lack of interpretation, and model comparison. In contrast to the previous studies that primarily deal with either segmentation or single CNN-based classification, the present work presents a universal comparative framework with numerous architectures and two heterogeneous datasets (Figshare and BraTS2020). It also incorporates attention-enhanced lightweight modeling (LeNet+SE) and explainable AI methods such as Grad-CAM and LIME to enhance trust in clinical practices and transparency. Moreover, cross-dataset validation can improve the generalization ability, and the proposed method becomes stronger, scalable, and applicable to the real-life scenario of brain tumor detection than the current methods.

TABLE VI. COMPARATIVE ANALYSIS BETWEEN EXISTING MODELS AND PROPOSED MODEL PERFORMANCE

| Models | Accuracy | References |
|--------------------------------------|--------------|------------|
| ResNet-50 | 81.6 | [33] |
| U-Net | 88.8 | [34] |
| Proposed LeNet +SE on Brats2020 Data | 98.44 | ----- |

This comparison makes it clear that the proposed model achieves better performance compared to other architectures. Although ResNet-50 and U-Net are powerful baseline models of deep learning and medical imaging, they do not have the combined advantages of attention-based feature enhancement and lightweight architecture optimization. The suggested method thus proves to be more accurate, learns

features better and is more appropriate in the classification of brain tumours in actual clinical practice.

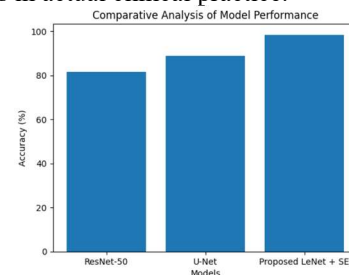


Fig. 20 Comparative Analysis

V. CONCLUSION

This paper provided a comparative deep learning brain tumor detection model based on MRI images with emphasis on comparing the existing CNN models with a proposed attention-enhanced lightweight model. The primary aim was to examine the performance of popular architectures like VGG16, ResNet50, AlexNet, and EfficientNetB0 and compare them with the proposed LeNet + SE model in a single experimental framework. The two heterogeneous datasets, Figshare and BraTS 2020, were employed to obtain a strong cross-dataset validation and the ability to measure the model generalization with different imaging conditions. The findings underscore the fact that, though traditional deep learning models are useful in terms of hierarchical features extraction using MRI data, they still have limitations with regard to generalization, computational efficiency as well as interpretability. The suggested LeNet +

SE model prevents these issues by incorporating Squeeze-and-Excitation attention schemes, which enhance the feature discrimination by emphasizing tumor-related areas and minimizing the needless computational complexity. Moreover, explainable AI models like Grad-CAM and LIME increase transparency and clinical believability in model prediction, the proposed model proves that lightweight architectures and attention mechanisms, combined with standardized testing across multiple datasets, can result in more robust and credible brain tumor classification. This research will help in the creation of efficacious, comprehensible, and clinically employable deep learning remedies to real-life medical imaging uses, enabling the enhancement of decision-making in health care systems.

REFERENCES

- [1] L. Velmurugan, R. K. Maheswari, K. Janani, K. Agalya, M. Poornima, and K. C. Gayathri, "Enhanced Framework for MRI Brain Tumor Recognition with Residual Learning and Intuitive Heatmap Visualization," *2024 Int. Conf. Innov. Comput. Intell. Commun. Smart Electr. Syst.*, no. March, pp. 1–7, 2025, doi: 10.1109/ICES63760.2024.10910526.
- [2] S. Saifullah, R. L. Drezewski, A. Yudhana, and A. P. Suryotomo, "Automatic Brain Tumor Segmentation: Advancing U-Net with ResNet50 Encoder for Precise Medical Image Analysis," *IEEE Access*, no. March, pp. 43473–43489, 2025, doi: 10.1109/ACCESS.2025.3547430.
- [3] M. A. L. Khaniki, M. Mirzaebonekhater, M. Manthouri, and E. Hasani, "Vision transformer with feature calibration and selective cross-attention for brain tumor classification," *Iran J. Comput. Sci.*, 2025, doi: 10.1007/s42044-024-00220-w.
- [4] X. Gu, Z. Shen, J. Xue, Y. Fan, and T. Ni, "Brain Tumor MR Image Classification Using Convolutional Dictionary Learning With Local Constraint," *Front. Neurosci.*, vol. 15, no. May, pp. 1–12, 2021, doi: 10.3389/fnins.2021.679847.
- [5] W. Zhang *et al.*, "Carbon dots: A future blood–brain barrier penetrating nanomedicine and drug nanocarrier," *Int. J. Nanomedicine*, vol. 16, pp. 5003–5016, 2021, doi: 10.2147/IJN.S318732.
- [6] F. Sauer *et al.*, "Whole tissue and single cell mechanics are correlated in human brain tumors," *Soft Matter*, vol. 17, no. 47, pp. 10744–10752, 2021, doi: 10.1039/d1sm01291f.
- [7] A. S. Kucheryavenko *et al.*, "Terahertz dielectric spectroscopy and solid immersion microscopy of ex vivo glioma model 101.8: brain tissue heterogeneity," *Biomed. Opt. Express*, vol. 12, no. 8, p. 5272, 2021, doi: 10.1364/boe.432758.
- [8] N. T. Singh, C. Kaur, P. Kaur, N. Kumari, and A. D. Chanu, "Machine Learning-based Disease Diagnosis in Healthcare: A Focus on Brain Tumor Detection," *Int. Conf. Recent Adv. Sci. Eng. Technol. ICRASET 2023*, no. October, pp. 1–6, 2023, doi: 10.1109/ICRASET59632.2023.10420375.
- [9] M. A. Gómez-Guzmán *et al.*, "Classifying Brain Tumors on Magnetic Resonance Imaging by Using Convolutional Neural Networks," *Electron.*, vol. 12, no. 4, pp. 1–22, 2023, doi: 10.3390/electronics12040955.
- [10] C. Heyn *et al.*, "Gadolinium Enhanced T2 FLAIR is an Imaging Biomarker of Radiation Necrosis and Tumor Progression in Patients with Brain Metastases," *Am. J. Neuroradiol.*, vol. 46, no. 1, p. ajnr.A8431, 2024, doi: 10.3174/ajnr.a8431.
- [11] R. Nimmagadda and P. K. Devi, "Optimized Deep Learning Framework for Brain Tumor Detection and Classification Using Hybrid Visual Geometry Group-16 With Reduced Weights Via Butterfly Optimization," *J. Theor. Appl. Inf. Technol.*, vol. 102, no. 16, pp. 6258–6279, 2024.
- [12] J. Madhumitha *et al.*, "Generative adversarial network with resnet discriminator for brain tumor classification," *Opsearch*, no. August, 2024, doi: 10.1007/s12597-024-00835-4.
- [13] S. Z. Kurdi, M. H. Ali, M. M. Jaber, T. Saba, A. Rehman, and R. Damaševičius, "Brain Tumor Classification Using Meta-Heuristic Optimized Convolutional Neural Networks," *J. Pers. Med.*, vol. 13, no. 2, 2023, doi: 10.3390/jpm13020181.
- [14] J. Chathumina and K. Jayakumar, "Enhancing Brain Tumor Diagnosis: A Comparative Review of Systems with and without eXplainable AI," *2024 5th Inf. Commun. Technol. Conf. ICTC 2024*, no. November, pp. 309–313, 2024, doi: 10.1109/ICTC61510.2024.10601680.
- [15] S. M. Alhtani *et al.*, "Improved Brain Tumor Segmentation and Classification in Brain MRI With FCM-SVM: A Diagnostic Approach," *IEEE Access*, vol. 12, no. April, pp. 61312–61335, 2024, doi: 10.1109/ACCESS.2024.3394541.
- [16] R. Hatae *et al.*, "Enhancing CAR-T cell metabolism to overcome hypoxic conditions in the brain tumor microenvironment," *JCI Insight*, vol. 9, no. 7, 2024, doi: 10.1172/jci.insight.177141.
- [17] W. J. Shelton *et al.*, "Long-read sequencing for brain tumors," *Front. Oncol.*, vol. 14, no. June, pp. 1–16, 2024, doi: 10.3389/fonc.2024.1395985.
- [18] Z. Jia and D. Chen, "Brain Tumor Identification and Classification of MRI Images Using Deep Learning Techniques," *IEEE Access*, vol. 13, no. July, pp. 123783–123792, 2025, doi: 10.1109/ACCESS.2020.3016319.
- [19] M. S. D. Devi, C. Shashank, B. D. Kumar, and K. Akash, "Detection of Brain Tumor Using Deep Learning Algorithm," *AIP Conf. Proc.*, vol. 3137, no. 1, pp. 29–47, 2025, doi: 10.1063/5.0264203.
- [20] A. Vandana, V. K. Sree, S. S. Charan, and J. K. Raju, "Brain Tumor Detection and Classification using Deep Learning," *14th Int. Conf. Adv. Comput. Control. Telecommun. Technol. ACT 2023*, vol. 2023-June, no. February, pp. 198–203, 2023, doi: 10.48175/ijarsct-3937.
- [21] M. Aggarwal, A. K. Tiwari, M. P. Sarathi, and A. Bijalwan, "An early detection and segmentation of Brain Tumor using Deep Neural Network," *BMC Med. Inform. Decis. Mak.*, vol. 23, no. 1, pp. 1–12, 2023, doi: 10.1186/s12911-023-02174-8.
- [22] M. Ravinder *et al.*, "Enhanced brain tumor classification using graph convolutional neural network architecture," *Sci. Rep.*, vol. 13, no. 1, pp. 1–22, 2023, doi: 10.1038/s41598-023-41407-8.
- [23] H. A. Shah, F. Saeed, S. Yun, J. H. Park, A. Paul, and J. M. Kang, "A Robust Approach for Brain Tumor Detection in Magnetic Resonance Images Using Finetuned EfficientNet," *IEEE Access*, vol. 10, pp. 65426–65438, 2022, doi: 10.1109/ACCESS.2022.3184113.
- [24] A. H. Khan *et al.*, "Intelligent Model for Brain Tumor Identification Using Deep Learning," *Appl. Comput. Intell. Soft Comput.*, vol. 2022, 2022, doi: 10.1155/2022/8104054.
- [25] M. Rizwan, A. Shabbir, A. R. Javed, M. Shabbir, T. Baker, and D. Al-Jumeily Obe, "Brain Tumor and Glioma Grade Classification Using Gaussian Convolutional Neural Network," *IEEE Access*, vol. 10, pp. 29731–29740, 2022, doi: 10.1109/ACCESS.2022.3153108.
- [26] L. Gaur, M. Bhandari, T. Razdan, S. Mallik, and Z. Zhao, "Explanation-Driven Deep Learning Model for Prediction of Brain Tumour Status Using MRI Image Data," *Front. Genet.*, vol. 13, no. March, pp. 1–9, 2022, doi: 10.3389/fgene.2022.822666.
- [27] S. Asif, W. Yi, Q. U. Ain, J. Hou, T. Yi, and J. Si, "Improving Effectiveness of Different Deep Transfer Learning-Based Models for Detecting Brain Tumors From MR Images," *IEEE Access*, 2022, doi: 10.1109/ACCESS.2022.3153306.
- [28] A. H. D. MO, and S. B., "Current challenges of the state-of-the-art of AI techniques for diagnosing brain tumor," *Mater. Sci. Eng. Int. J.*, vol. 7, no. 4, pp. 196–208, 2023, doi: 10.15406/mseij.2023.07.00224.
- [29] R. Yousef *et al.*, "U-Net-Based Models towards Optimal MR Brain Image Segmentation," *Diagnostics*, vol. 13, no. 9, 2023, doi: 10.3390/diagnostics13091624.
- [30] M. Martucci *et al.*, "Magnetic Resonance Imaging of Primary

- Adult Brain Tumors: State of the Art and Future Perspectives,” *Biomedicines*, vol. 11, no. 2, 2023, doi: 10.3390/biomedicines11020364.
- [31] A. R. Venmathi, S. David, E. Govinda, K. Ganapriya, R. Dhanapal, and A. Manikandan, “An Automatic Brain Tumors Detection and Classification Using Deep Convolutional Neural Network with VGG-19,” *2nd Int. Conf. Adv. Electr. Electron. Commun. Comput. Autom. ICAECA 2023*, no. June, pp. 1–5, 2023, doi: 10.1109/ICAECA56562.2023.10200949.
- [32] M. T. R. Shawon, G. M. S. Shibli, F. Ahmed, and S. K. S. Joy, “Explainable Cost-Sensitive Deep Neural Networks for Brain Tumor Detection from Brain MRI Images considering Data Imbalance,” vol. 3, 2023.
- [33] R. K. Yadav, A. K. Mishra, D. K. Jang Bahadur Saini, H. Pant, R. G. Biradar, and P. Waghodekar, “A Model for Brain Tumor Detection Using a Modified Convolution Layer ResNet-50,” *Indian J. Inf. Sources Serv.*, vol. 14, no. 1, pp. 29–38, 2024, doi: 10.51983/ijiss-2024.14.1.3753.
- [34] T. A. Samee, Nagwan Abdel and A. Rizwan, “Clinical Decision Support Framework for Segmentation and Cascaded Learning Algorithm,” *Healthcare*, 2022.